Edinburgh 99/11
September 1999

The topological susceptibility in 'full' (UK)QCD.

A. Hart[a] and M. Teper[b].

[a]Dept. of Physics, University of Edinburgh, King's Buildings, Edinburgh EH9 3JZ, Scotland.

[b]Theoretical Physics, University of Oxford, 1 Keble Road, Oxford OX1 3NP, England.

We report first calculations of the topological susceptibility measured using the field theoretic method on SU(3) gauge configurations produced by the UKQCD collaboration with two flavours of dynamical, improved, Wilson fermions. Using three ensembles with matched lattice spacing but differing sea quark mass we find that hybrid Monte Carlo simulation appears to explore the topological sectors efficiently, and a topological susceptibility consistent with increasing linearly with the quark mass.

The latest UKQCD runs generate SU(3) field configurations using a Wilson gauge action coupled to $n_f = 2$ flavours of Wilson sea quarks, non–perturbatively improved such that the leading order discretisation errors in spectral quantities should be $\mathcal{O}(a^2)$. In dynamical simulations the lattice spacing, a, is influenced by the gauge coupling, β, and the quark mass parameter, κ. The ensembles studied represent three points on a trajectory in the (β, κ) space of (approximately) constant a and physical volume ($Va^4 = 16^3.32a^4$) [1]. [The lattice spacing has been defined from the static inter–quark potential, using $r_0 = 0.49$ fm [2].] Along such trajectories, however, there is a change in chiral behaviour as seen in the pseudoscalar to vector mesonic mass ratio in Table 1. [Dimensionless lattice quantities are denoted with circumflexes throughout.]

We measure the topological charge density on the lattice using the field theoretic operator

$$\hat{Q}(n) = \frac{1}{2} \times \frac{1}{16} \varepsilon^{\pm}_{\mu\nu\sigma\tau} \, \mathrm{Tr} \, U_{\mu\nu}(n) U_{\sigma\tau}(n), \qquad (1)$$

symmetrised such that $\varepsilon^{\pm}_{\mu\nu\sigma,-\tau} = -\varepsilon^{\pm}_{\mu\nu\sigma,+\tau}$ *etc.* to improve the signal on moderately cooled lattices. The topological charge, $\hat{Q}$, and susceptibility, $\hat{\chi}$, are then

$$\hat{Q} = \frac{1}{32\pi^2} \sum_n \hat{Q}(n) \qquad \hat{\chi} = \frac{\langle \hat{Q}^2 \rangle}{V}. \qquad (2)$$

Although formally in the weak coupling limit $\hat{Q}$ is related to that of the continuum by $\hat{Q} = a^4 Q + \mathcal{O}(a^6)$, the prefactors of the higher order terms typically have momenta on the scale of $1/a$ such that they are $\mathcal{O}(1)$, and $\hat{Q}$ becomes increasingly dominated by ultraviolet noise near the continuum limit. It is also subject to a multiplicative renormalisation that reduces the signal at the β couplings accessible to simulation.

An established, and well understood, procedure to extract the topological signal is to cool the configurations prior to measuring $\hat{Q}$. This locally smoothens the lattice fields to remove the ultraviolet fluctuations, and drives the renormalisation constant to unity. We move through the lattice links in a staggered fashion, updating each Cabibbo–Marinari subgroup in turn so as to exactly minimise the SU(2) Wilson plaquette action. This action is the most local and thus is expected to do least damage to correlation functions on physical length scales. Updating every link once corresponds to one cooling 'sweep'.

Such a cooling action, however, also destroys topological features when applied *in extremis*. Instanton–anti-instanton pairs in the vacuum are

β	5.20	5.26	5.29
κ	0.1350	0.1345	0.1340
No. cfgs.	150	100	100
$\hat{r}_0$	4.58 (8)	4.58 (6)	4.45 (6)
$\frac{\hat{m}_\pi}{\hat{m}_\rho}$	0.69 (1)	0.79 (1)	0.83 (1)

Table 1
Lattice spacing and pion to rho mass ratios [3].

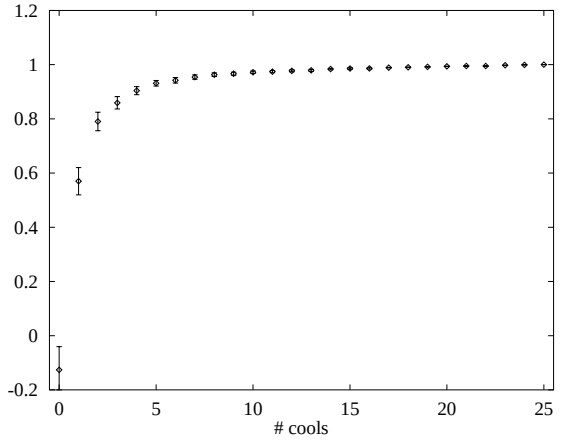

Figure 1. Normalised $\langle \hat{Q}(n_c) \cdot \hat{Q}(25) \rangle$ versus the number of cools, n_c, at $\beta = 5.20$.

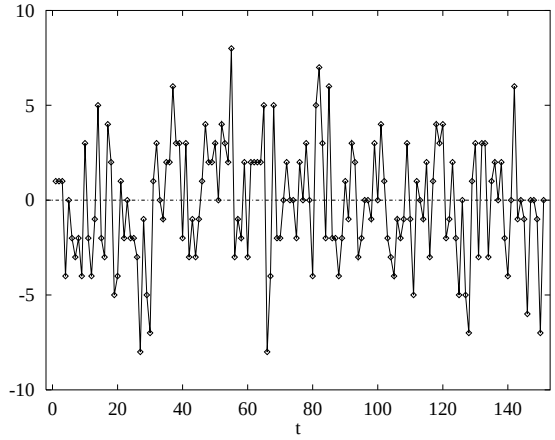

Figure 2. $\hat{Q}(n_c = 10)$ vs. simulation time in units of 40 HMC trajectories at $\beta = 5.20$.

not stable minima of the action (even in the continuum) and under cooling there is an attractive force leading to annihilation. Whilst this is an issue in measurements of instanton size distributions, there in no net change in the topological charge and the susceptibility is thus stable.

The lattice regularisation breaks scale invariance, and the Wilson action of an instanton is an increasing function of the core size, ρ. (Isolated) instantons shrink and disappear under cooling, leading to a net change in $\hat{Q}$ and $\hat{\chi}$. Whilst such events may be monitored in relatively smooth configurations, it is still desirable to perform as few cooling steps as possible to expose the signal before making measurements. In Fig. 1 we plot the normalised correlation between the topological charge after a given number of cooling sweeps, n_c, relative to that after $n_c = 25$:

$$\frac{\langle \hat{Q}(n_c) \cdot \hat{Q}(25) \rangle}{\frac{1}{2}\left(\langle \hat{Q}(n_c) \rangle^2 + \langle \hat{Q}(25) \rangle^2 \right)} \tag{3}$$

We find remarkable stability in $\hat{Q}$ from 5 cooling sweeps out to at least 25 cooling steps.

One technical point of interest is the rate at which configurations become topologically independent under Monte Carlo updating; the topological charge is related to the small eigenvalues of the fermion matrix and should be one of the slowest modes to decorrelate. We show a Monte Carlo time history plot for our most chiral ensemble in Fig. 2, and we estimate the integrated autocorrelation times in units of the 40 HMC trajectories between configurations in Table 2, albeit using a small ensemble, indicating pretty good decorrelation at these quark masses. We note that autocorrelation times are longer for the larger β ensembles despite these being the less chiral.

Also of issue is the ergodicity of the MC update. Measuring $\hat{Q}$ over the whole configuration we find the ensemble averages to be within ~ 1.5 (relatively large) standard deviations of zero in Table 2, and Fig. 3 shows a relatively Gaussian sampling of the topological sectors.

In the continuum, the topological charge of a configuration is integer. On the lattice this is not so, nor is the charge measured using our operator on a configuration particularly close to integer. This can be attributed to the presence of narrow instantons whose charge is significantly less than unity. Attempts can be made to calibrate and correct for this [4] but we defer application of such procedures until [5]. We have both maintained the charge as a non–integer for the purposes of calculating the topological susceptibility, and also rounded the value on each configuration to the nearest integer, and found that the topological susceptibilities obtained are consistent within statistical errors.

In Table 2 we show our estimates for the topo-

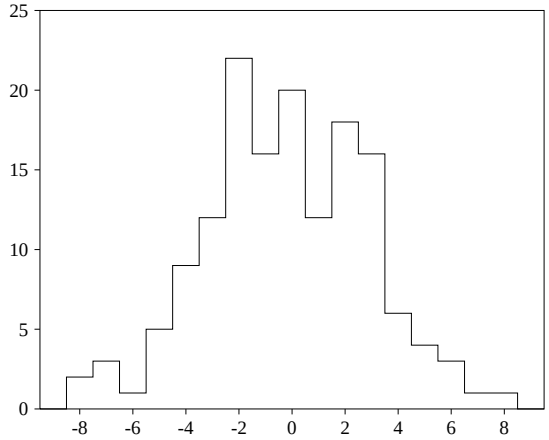

Figure 3. Histogram of $\hat{Q}^{\rm int}$ at $n_c = 10$ on the $\beta = 5.20$ ensemble.

logical susceptibility measured after 25 cooling sweeps. In the chirally broken, confining phase at low temperatures, the sea quarks induce an attractive interaction which leads to instanton–anti-instanton pairing and a suppression of the topological susceptibility as the dynamical quark mass is lowered:

$$\chi = \frac{m_q \langle \bar{\psi}\psi \rangle}{n_f^2} + \mathcal{O}(m_q^2) \tag{4}$$

where $\langle \bar{\psi}\psi \rangle$ is summed over light quark flavours, and should be evaluated in the $m_q \to 0$ limit. The quark mass is not known *a priori* but may be re-expressed in terms of the pseudoscalar decay constant using the PCAC relation $m_q \langle \bar{\psi}\psi \rangle = f_\pi^2 m_\pi^2$ such that for sufficiently chiral sea quarks, the topological susceptibility should be quadratic in the pseudoscalar mass and decay constant:

$$\chi = \frac{f_\pi^2 m_\pi^2}{n_f^2} + \mathcal{O}(m_\pi^4). \tag{5}$$

β	$\tau_{\rm int}^{\rm est.}$	$\langle \hat{Q} \rangle$	$\hat{\chi}^{\rm int} \cdot 10^5$
5.20	0.71 (41)	0.03 (56)	7.5 (1.4)
5.26	0.67 (28)	−0.47 (28)	7.2 (1.5)
5.29	1.5 (1.2)	1.10 (97)	14.8 (2.3)

Table 2
Mean $\hat{Q}$, autocorrelation time and the topological susceptibility at $n_c = 25$.

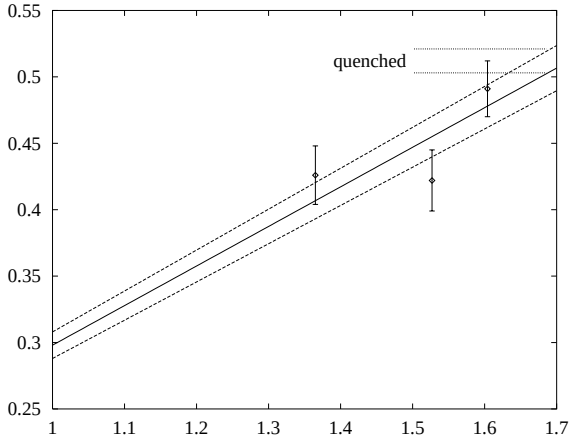

Figure 4. $\hat{r}_0 (\hat{\chi}^{\rm int})^{\frac{1}{4}}$ vs. $\sqrt{\hat{r}_0 \hat{m}_\pi}$ with a linear fit.

In Fig. 4 we plot the susceptibility versus the pseudoscalar mass in units of r_0, and find the data are consistent with such a leading order fit through the origin. We may use the fitted slope of this graph to provide an estimate of the pseudoscalar decay constant, finding it to be very low compared to the experimental value.

Although such an estimate must be regarded as preliminary given the volume of data so far analysed, it is clear from Fig. 4 that the heaviest of our sea quark masses yields a topological susceptibility that is in statistical agreement with the quenched value, and attempting to fit the leading order chiral behaviour to this point is likely to lead to an underestimate of f_π; $\mathcal{O}(m_q^2)$ terms are likely to be large, including the effects of not extrapolating $\langle \bar{\psi}\psi \rangle$ to $m_q \to 0$. Ongoing analysis of further configurations at these and lighter sea quark masses should clarify the situation.

REFERENCES

1. A. Irving *et al.*, Phys. Rev. D 58 (1998) 114504 [hep-lat/9807015].
2. R. Sommer, Nucl. Phys. B 411 (1994) 839 [hep-lat/9310022].
3. J. Garden *et al.*, these proceedings [hep-lat/9909066].
4. D. Smith and M. Teper, Phys. Rev. D 58 (1998) 014505 [hep-lat/9801008].
5. A. Hart and M. Teper, in progress.

Acknowledgments.

A.H.'s work was supported in part by United Kingdom PPARC grant GR/K22744, and that of M.T. by grants GR/K55752 and GR/K95338.